JOURNAL OF MATERIALS SCIENCE 11 (1976) 1125–1134

Structure and mechanical properties of unidirectionally solidified Zn-Ge eutectic alloys

M. SAHOO, R. W. SMITH
Metallurgical Engineering Department, Queen's University, Kingston, Ontario, Canada

The Al–Si eutectic alloys are known to undergo various structural transitions when unidirectionally solidified. This paper describes another metal/non-metal combination, Zn–Ge, which undergoes closely similar morphological changes. The tensile and compressive properties of the unidirectionally solidifed Zn–Ge eutectic have been examined and compared with those of the Al–Si eutectic. It is shown that the marked compressional stiffness of Al–Si alloys containing ⟨1 0 0⟩ type branched silicon dendrites only arises because of the lateral constraints of the aluminium matrix and does not occur in the Zn–Ge system.

1. Introduction

Eutectics display a wide variety of microstructural forms, some of which appear to offer potential applications as composite materials in engineering and other applications. In binary alloys at least, the authors [1–3] have shown that the often confusing array of morphologies may be reduced to an orderly arrangement by distinguishing various characterizing "parameters", namely the entropy of solution (ΔS) of each phase and the volume fraction (V_f) of the minor constituent. If ΔS is small for both phases, regular rod or lamellar structures form which tend to be insensitive to changes in freezing rate (R) during solidifcation. However, should ΔS for the minor constituent exceed some critical value (5.5 cal K^{-1} mol^{-1}), then the phase tends to facet. This causes the resulting microstructure to be markedly dependent on the rate at which it froze and the particular V_f value for the system. Since many common industrial alloys are in this group, e.g. Al-Si, Fe–C, a broad study of the mechanical properties of binary eutectics is in progress in the author's laboratory.

As noted above, non-faceted/faceted (nf/f) eutectics may be characterized from a microstructural viewpoint in terms of V_f. Thus the various forms (of silicon) appearing in Al–Si alloys may be observed as a general feature of eutectics in which $V_f \approx 6$ to 18%. In that the crystal structures of the various eutectic phases appearing in alloys in this group (and others) vary, it is of interest to determine whether any similarly broad classification of mechanical properties can be produced.

The mechanical properties of unidirectionally frozen Al–Si alloys have been examined in tension [4–5] and compression [5]. To continue this study it was then necessary to investigate the effect of changing the structure of the matrix. Of the hcp elements easily available, Zn–Si and Cd–Si display little or no miscibility, and magnesium forms a silicide. In view of this, germanium systems were examined, in substitution for those of silicon, since silicon and germanium terminal-solid-solutions might be expected to behave similarly. Of these, only Zn–Ge appeared suitable since it has the appropriate volume fraction, 7 vol%, and so displays closely similar growth morphologies [3]. Thus the following is a description of a study of the mechanical properties of Zn–Ge eutectic alloys from which it will be seen that this alloy closely resembles Al–Si in both morphology and mechanical properties.

2. Experimental

Zn–Ge eutectic alloys with a nominal germanium content of 6 wt% were prepared from 99.999% pure elemental materials. Weighed amounts of Zn and Ge were encapsulated in argon-filled pyrex tubes, heated in a gas flame to melt the constituents and shaken vigorously to enourage complete mixing. The solidifed rods were swaged to 6 mm and 5 mm diameter to promote macrohomogeneity. The 5 m diameter rods were sealed into argon-filled 6 mm I.D. pyrex tubes and directionally solidified by lowering into a water jacket. This enabled temperature gradients of approximately 10° C mm^{-1} to be obtained. Since the Al–Si alloys reported in [5] were directionally solidified horizontally under argon in a split graphite mould, water cooled at one end, some of the 6 mm diameter Zn–Ge rods were directionally solidified also under the same growth conditions.

The first and last 3 cm of each alloy were rejected and the tensile and compressive testing specimens were cut from the remainder. Longitudinal and transverse sections were prepared for metallographic examination.

Specimens for tensile testing were machined in a jeweller's lathe to produce a reduced diameter of 3.8 mm. Compression specimens, ~ 12 mm long and 5 and 6.3 mm in diameter, were carefully polished to produce parallel faces and then etched to remove any worked layer. All tensile and compressive tests were performed at ambient temperatures (~ 25° C) with the stress axis parallel to the growth axis, using an Instron testing machine at a cross-head speed of ~ 0.13 mm min^{-1}. In the case of tensile tests, specimen elongations were obtained from the cross-head movement of the Instron testing machine.

Metallographic specimens were mounted using a cold mounting technique, polished in the conventional manner and etched with a solution of 5 ml conc. HCl and 95 ml ethanol. A Phillips AMR 900 Scanning Electron Microscope (SEM) was used to examine both the as-grown and deformed microstructure. The orientation of the matrix was examined using X-ray pole-figure techniques.

3. Results and discussion

3.1. Al–Si [5]

Since the mechanical properties of the Al–Si eutectic alloys are to be used as reference points in discussing the mechanical properties of Zn–Ge, it would appear appropriate to summarize the former. Unidirectional solidification results in the following morphologies, as the rate of growth is increased: branched dendrites → complex-regular → irregular flaky forms → continuous (modified) fibrous forms. The quench-modified alloy exhibited maximum silicon refinement.

The U.T.S. of the eutectic was found to increase with the growth rate. Highest strengths (~ 220 N mm^{-2} or 32 000 psi) were obtained only in the quench-modified condition. When tested in compression, eutectics, directionally solidified at low growth rates, and consisting of ⟨1 0 0⟩ silicon dendrites, showed more promise of attaining high compressive strengths (up to about 500 N mm^{-2} or 72 000 psi) and minimum ductility (< 1%). However, specimens from other growth conditions showing complex-regular, irregular, and fibrous silicon morphologies did not fracture up to 20% compressive plastic strain.

3.2. Morphology

Returning to the Zn–Ge system, the sequential optical micrographs of Fig. 1 of transverse sections through Zn–6 wt% Ge eutectic alloys indicate that a variety of growth forms may occur as the growth rate is increased from a value of 2.7 mm h^{-1}.

In samples directionally solidifed at 2.7 and 5.4 mm h^{-1}, the germanium grew as branched dendrites (Fig. 1a). However, at the lowest growth rate, germanium was found to be present in a relatively massive form. This branched form is similar to that reported in Ag–Ge [6], Al–Si, Ag–Si and Au–Si systems [5, 7, 8]. Longitudinal section of the quenched growth front corresponding to the section in Fig. 1a suggests that the growth front is non-isothermal (Fig. 2). These features are identical to those of the Al–Si system and tend to indicate that germanium also grows with a preferred ⟨1 0 0⟩ texture. Longitudinal sections etched with C.P.4 solutions [9] revealed multiple twins running parallel to growth direction

With further increases in growth rate, the branched germanium rods were gradually modified although a few branched/unbranched plates were observed even at a growth rate of 160 mm h^{-1} (Fig. 1c).

At growth rates greater than 160 mm h^{-1}, the microstructure changed to a fibrous form (Fig. 1d) This figure shows the change in scale of the Ge distribution, and the presence of the zinc primaries. The microstructures observed in the chill-cast

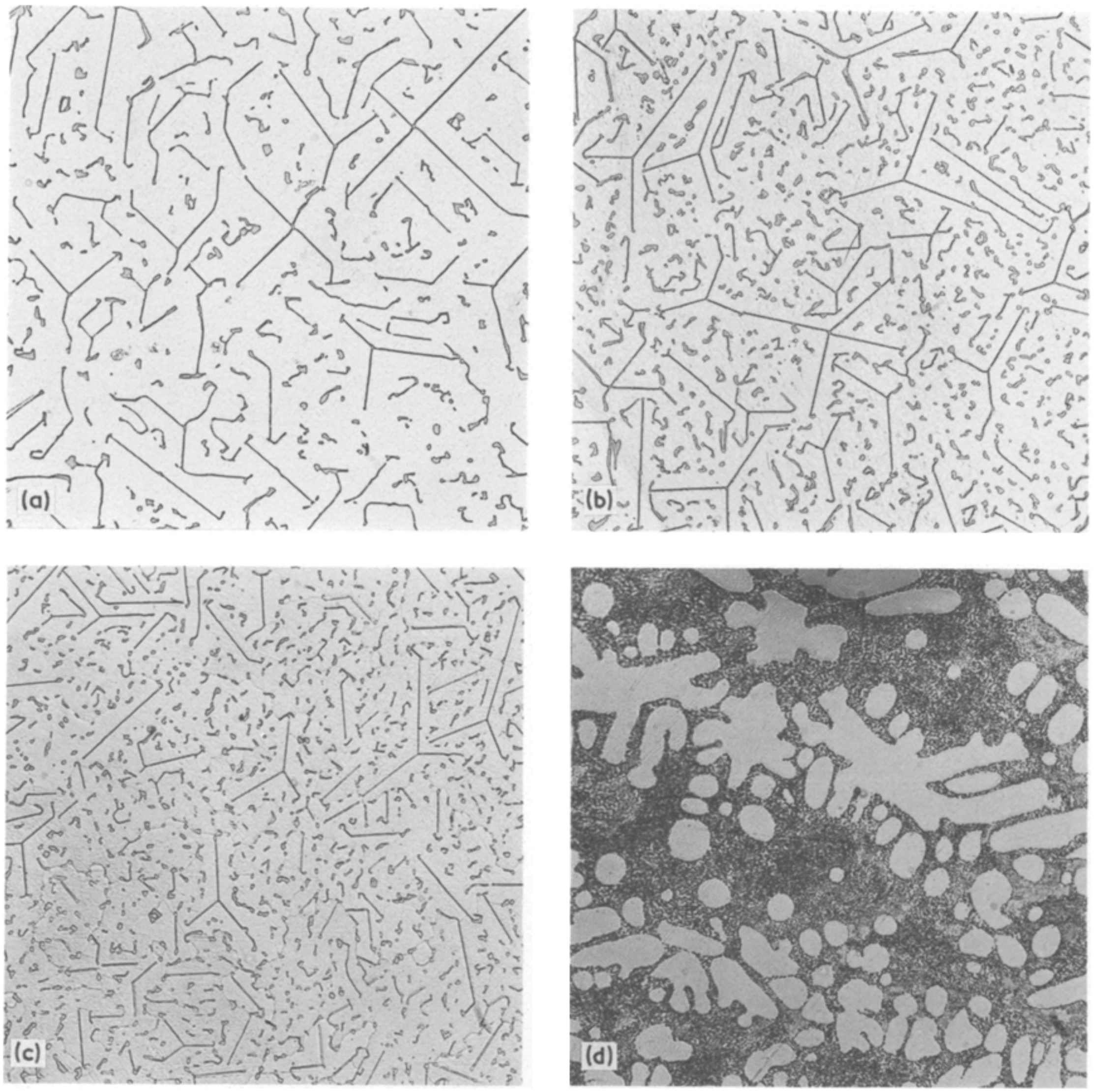

Figure 1 Optical micrographs of transverse sections through directionally solidified Zh–Ge eutectic alloys showing the Ge morphology at various growth rates. (a) $R = 5.4\,\mathrm{mm\,h^{-1}}$ (× 200); (b) $R = 16\,\mathrm{mm\,h^{-1}}$ (× 200; (c) $R = 160\,\mathrm{mm\,h^{-1}}$ (× 500); (d) $R = 4800\,\mathrm{mm\,h^{-1}}$ (× 500).

condition were not uniform. In some areas the appearance of the microstructure is similar to that produced in the Al–Si eutectic alloys in the chill-cast condition. However, in others the structure was much coarser, displaying many plate-like forms and angular fragments (Fig. 3). A scanning electron micrograph (Fig. 4) of the heavily etched longitudinal section of the modified Zn–Ge eutectic suggests that the germanium fibres are interconnected as with Al–Si modified alloys [10].

The grain-boundaries of the polycrystalline Zn matrix were revealed by etching with a solution of 320g CrO_3, 20g Na_2SO_4, and 1000ml H_2O and then examined under polarized light. The average grain diameter of the Zn matrix was greater than that of the aluminium matrix in equivalent Al–Si alloys by a factor of about 4.

It should be noted that the Zn–Ge eutectic did not exhibit either the complex-regular or the irregular flaky forms which are transition structures between the branched dendritic and the fibrous form of Si in Al–Si eutectic alloys. The coarse irregular flaky form of Si is also the normal sand-cast structure of the Al–Si eutectic alloys. In order to see if such flaky structure can be

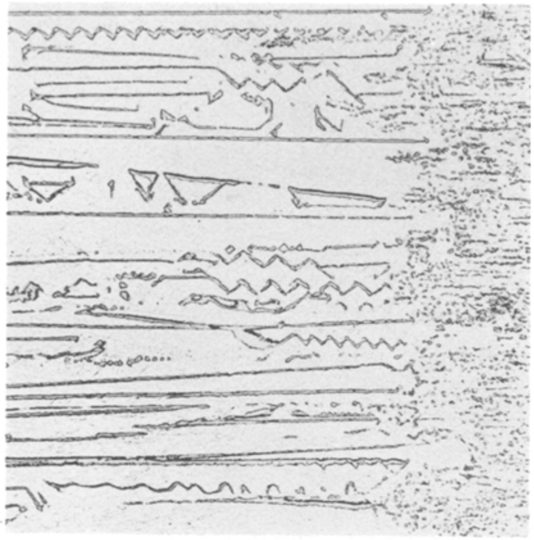

Figure 2 Optical micrographs of longitudinal section through quenched growth front corresponding to microstructure of Fig. 1a (X 110).

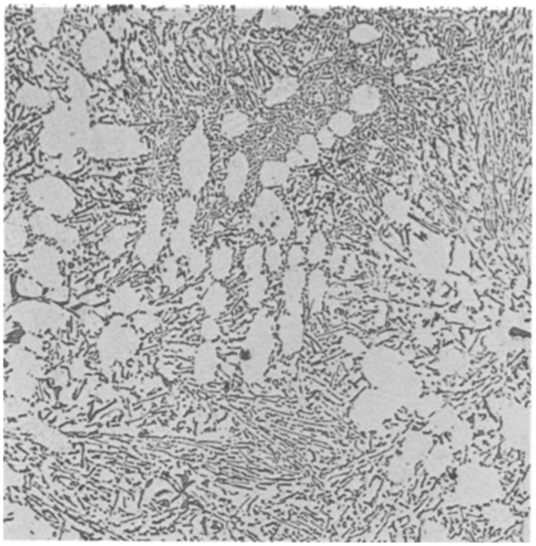

Figure 3 Optical micrograph of sodium-free Zn–Ge eutectic alloy in the chill cast condition (X 500).

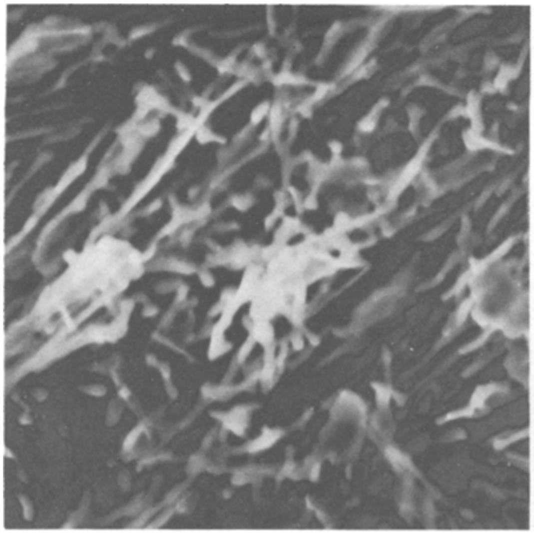

Figure 4 Scanning electron micrograph of Zn–Ge eutectic alloy directionally solidified at 4800 mm h^{-1} (X 5000).

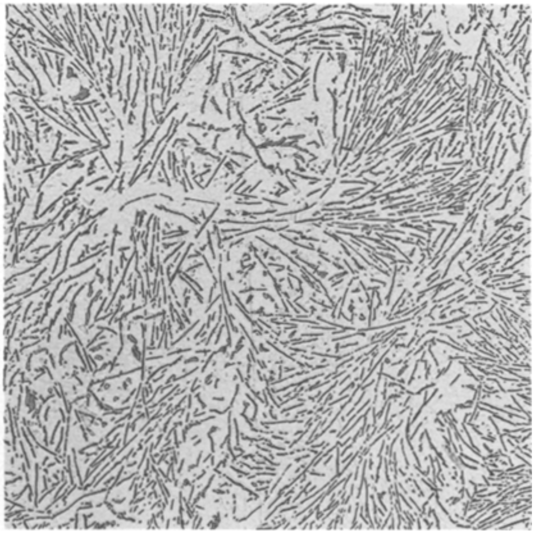

Figure 5 Optical micrograph of Zn–Ge eutectic alloy cast in preheated ceramic mould (X 200).

produced in Zn–Ge alloys, eutectic alloys with off-eutectic compositions, hypo- and hyper-eutectic alloys were cast in pre-heated ceramic moulds. The cast structure of hypo-eutectic (4.5 wt% Ge) and eutectic alloys contained irregular flaky form of Ge in the centre of the castings (Fig. 5). The hyper-eutectic alloys (7.5 wt% Ge) exhibited such flaky structure throughout the casting. The complex-regular form of Ge was also observed in this alloy. This led to the suggestion that the lower volume fraction combined with the absence of favourable G/R values, (G = temperature gradient, R = rate of growth) hindered the development of well-defined flakes in the eutectics directionally solidifed at a growth rate of 160 mm h^{-1}. This possibility was verified by directionally solidifying the Zn–Ge eutectic over a range of G/R values at a fixed growth rate of 160 mm h^{-1}, the normal green-sand rate of solidification. The temperature gradient was varied by changing the temperature of the furnace from which the specimen was lowered. It was observed that at very low G values (superheat = 27° C, $C = 1.5$° C mm^{-1}), the irregular form of Ge was observed throughout the length of the specimen. At increasingly higher G values, the first 40 to 50 mm of the specimen exhibited a flaky form of Ge which then changed to a modified form as shown in Fig. 1c.

The flaky form of Ge was found to be modified to a fibrous form by the addition of about 0.05 wt% elemental sodium added to the melt prior to the casting in a pre-heated ceramic mould. Fig. 6 is the optical micrograph of the sodium-modified eutectic alloy. The eutectic channelling seen in this micrograph has been observed in over-modified Al–Si alloys [11]. Figs. 7 and 8 are the scanning electron micrographs of the unmodified and sodium-modified Zn–Ge eutectic alloys corresponding to Figs. 5 and 6 respectively.

Comparing Figs. 4 and 8 it can be concluded that the morphology of the Ge phase in both the quench-modified and the sodium-modified condition is similar.

The sodium content of the sodium-modified

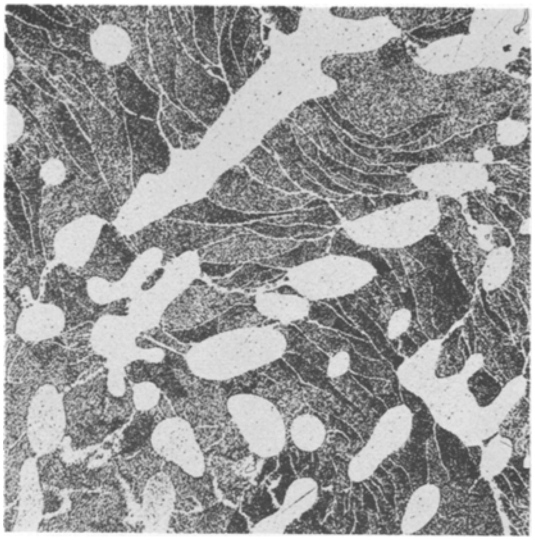

Figure 6 Optical micrograph of the sodium-modified Zn–Ge eutectic showing channelling of the matrix (× 200).

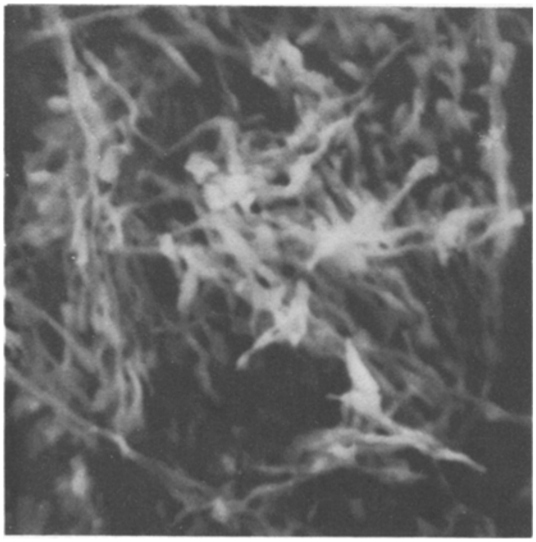

Figure 8 Scanning electron micrograph of the sodium-modified Zn–Ge eutectic corresponding to Fig. 6 (× 5000).

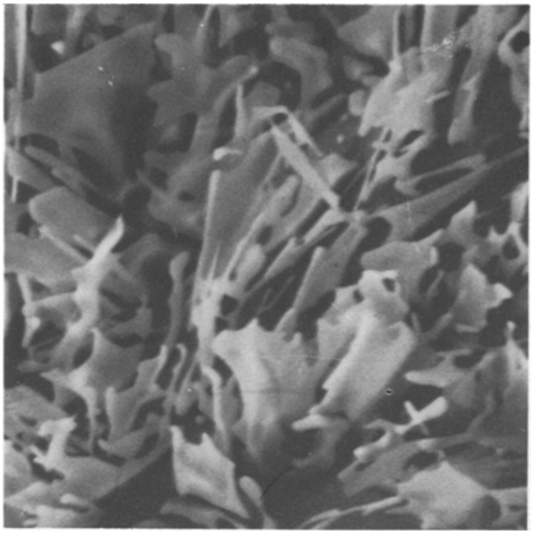

Figure 7 Scanning electron micrograph of the unmodified Zn–Ge eutectic corresponding to Fig. 5 (× 2000).

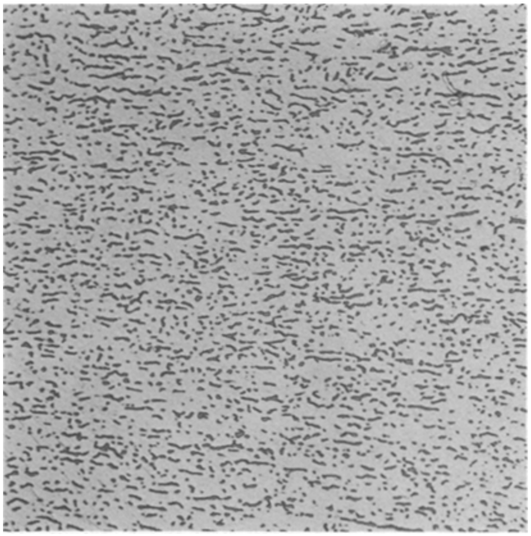

Figure 9 Optical micrograph of the longitudinal section of the sodium-modified Zn–Ge eutectic directionally solidified at 160 mm h^{-1} (× 500). The sodium content of the eutectic was reduced by mixing the modified alloy corresponding to Fig. 6 with some unmodified alloy.

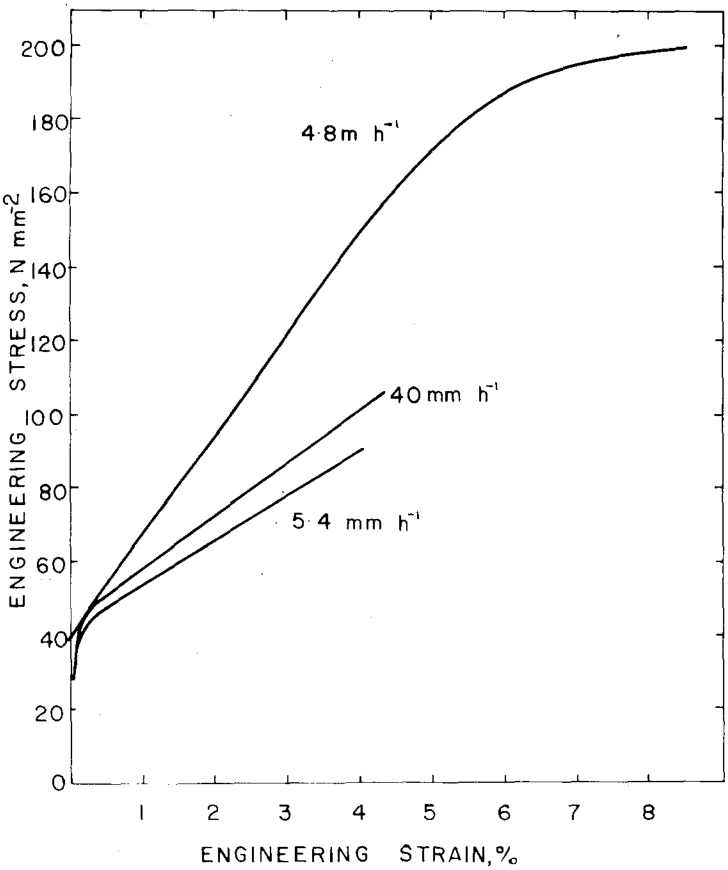

Figure 10 Typical tensile stress/strain curves for the unidirectionally solidified Zn–Ge eutectic alloys.

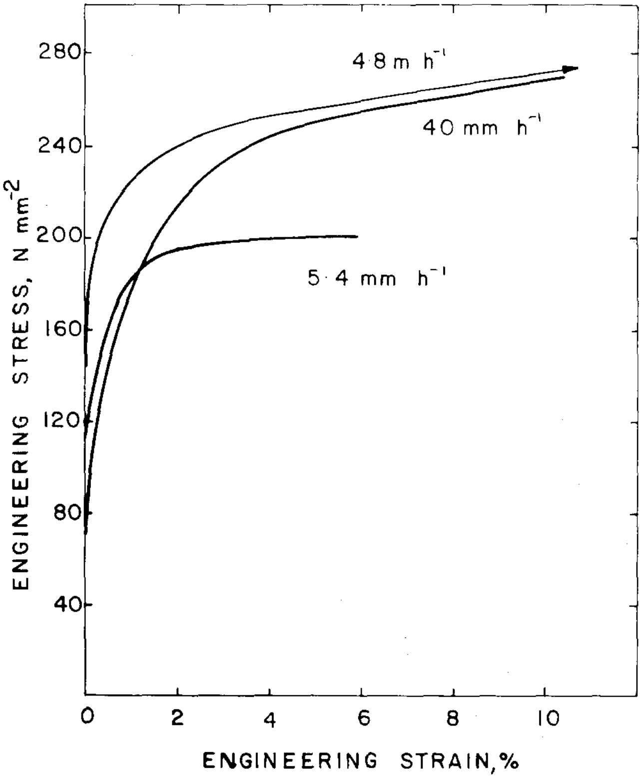

Figure 11 Typical compressive stress/strain curves for the unidirectionally solidified Zn–Ge eutectic alloys. Specimen ends were not lubricated.

TABLE I Room temperature mechanical properties of directionally solidified Zn–Ge alloys

	Tension			Compressions		
Growth rate (mm h^{-1})	0.2% offset yield strength (N mm^{-2})	U.T.S. (N mm^{-2})	fracture strain (%)	0.2% offset yield strength (N mm^{-2})	U.T.S. (N mm^{-2})	% uniform elongation
2.7	†44.5	110	6.9	153	264	2.8
				155	259	2.5
				144*	263*	2.5*
5.4	†40.0	92	4.0	139	200	5.7
				139	208	5.3
				141	212	5.7
				116*	208*	3.2*
16.0	†44.5	101	4.0	114	235	13.1
				112	224	14.0
				95*	217*	8.9*
40.0	†55.0	109	1.4	122	275	10.0
	47.5	103	4.2	121	260	14.0
				118*	255*	12.7*
	45.8	105	4.5	117	269	10.2
				104*	261*	10.6*
160.0	67.0	124	1.6	–	–	–
	51.7	138	2.5	124	282	12.6
				139	288	9.2
				125*	256*	11.6
200.0	54.5	176	13.9	155	276	8.2
1600.0	51.5	179	7.3	185	269	10.9
				199	275	10.3
				171*	253*	8.6*
2000.0	41.0	200	8.9	226	310	10.2
				200	290	11.5
				184*	280*	13.3*
4800.0	46.8	200	8.8	200	287	20.0
				197	290	27.0
				181*	255*	5.0*
chill cast	54.5	150	5.3	166*	285*	15.6*
160.0 (sodium-modified)	47.0	188	12.5	–	–	–
	47.0	188	10.0	–	–	–

* Specimen ends were lubricated with Teflon.

† Horizontally solidifed.

Zn–Ge eutectic was reduced by mixing it with some unmodified alloy and then directionally solidifying at a growth rate of 160 mm h^{-1}. Fig. 9 is the optical micrograph of the directionally solidified eutectic. This micrograph does not show the eutectic channelling. However, the structure remains modified.

3.3. Mechanical properties

The tensile and compressive properties of the Zn–Ge eutectics are summarized in Table I. Typical room temperature stress–strain curves are shown in Figs. 10 and 11.

3.3.1. Tensile properties

Table I shows that at the lowest growth rate when Ge appears in a massive and branched dendritic form, the eutectic has a U.T.S. of 110 N mm^{-2} or 16 000 psi. Further increases in growth rates up to 160 mm h^{-1} did not produce significant changes in its mechanical properties in spite of the fact that the Ge phase became gradually finer. At higher growth rates, the U.T.S. of the eutectic reached a value of 200 N mm^{-2} or 29 000 psi. This corresponds to almost two-fold increases in strength due to modification of the microstructure The U.T.S. of the sodium-free chill-cast material, however, was only 150 N mm^{-2} or 22 000 psi. This marked decrease in strength is attributed to the stress-raising effect of the irregularity shaped Ge particles.

The tensile strength of the sodium-modified Zn–Ge eutectic, directionally solidifed at a growth rate of 160 mm h^{-1}, was 188 N mm^{-2} or 27 000 psi, in approximate agreement with the tensile strength of the sodium-free eutectic directionally solidifed at fast growth rates. It was noted that the sodium-modified Zn–Ge eutectic alloys, case in pre-heated ceramic moulds, often broke when machining into tensile specimens. This was attributed to the over-modification of the Ge phase, corresponding to Fig. 6.

The tensile properties of the Zn–Ge eutectic closely resemble those of the Al–Si eutectic in spite of the fact that the volume fraction of the non-metallic phase in the latter is almost double than that in the former. In addition, the crystal structures of the polycrystalline matrix in these two-phase alloys are different. The fine-grained matrix in Al–Si has an fcc structure and undergoes rapid work-hardening due to the operation of polyslip in each grain. By contrast, the hcp Zn matrix in the Zn–Ge eutectic has a coarse grain structure, having 4 to 6 grains per crosssection. Thus Zn deforms as a "multicrystal" rather than a "polycrystal" and the mechanical properties of the Zn matrix tend to be independent of grain size [12]. Since the number of slip systems available to the Zn matrix is likely to be less than that required for completely homogeneous deformation, the stress–strain curves for the Zn–Ge eutectic would not be expected to exhibit the rapid work-hardening associated with the deformation of Al–Si. In fact, the curves depict almost single crystal deformation (c.f. Fig. 2 of [5]). This results from the fact, confirmed by X-rays, that at small growth rates, the zinc has a $\langle 0\,0\,0\,1 \rangle$ texture, with a progressive rotation away from the crystal axis as R is increased.

The highest strength achieved in the Al–Si eutectic was 220 N mm^{-2} or 29 000 psi. This is almost double the U.T.S. of fine-grained zinc of 99.999% purity [13, 14]. It should be remembered that this eutectic contains only 7 vol% of the Ge phase.

By analogy with the Al–Si eutectic, the fibrous form of the Zn–Ge alloys can be characterized as a potential fibre-reinforced composite. The criteria for fibre reinforcement have been discussed in [5, 15, 16]. The modulus of elasticity for polycrystalline Zn is 9250 N mm^{-2} or 13.4×10^6 psi [17]. In case of Ge, $E_{\langle 100 \rangle} = 10\,300$ N mm^{-2} or 15×10 psi and $E_{\langle 111 \rangle} = 15\,500$ N mm^{-2} or 22.5×10^6 psi [18]. Thus it is reasonable to assume that for Ge, $E > 10\,300$ N mm^{-2} or 15×10^6 psi. Hence Ge fibres are expected to provide composite reinforcement in the zinc matrix. The fracture stress of [1 1 1] Ge whiskers is about 1300 N m^{-2} or 190 000 psi [19]. It has also been reported that the fracture stress of germanium can be increased [20] to a much higher value of 2050 N mm^{-2} or 427 000 psi when tested in CP-4 solution (to remove surface cracks). Thus it would appear that effective load transfer from the matrix to the Ge fibres to achieve fibre reinforcement can take place.

The tensile strength of the composite, estimated from the rule of mixtures [15], is of the order of 156 N mm^{-2} or 22 600 psi for a fibrous strength of (σ_f) of 1300 N mm^{-2} or 190 000 psi and a matrix strength (σ_m) of 69 N mm^{-2} or 10 000 psi [13]. This is slightly less than the experimentally measured value for the modified eutectics. However, when using the rule of mixtures in predicting the tensile strength of composites, two important factors should be taken into consideration. The first, and perhaps the most important of these is the matrix constraints due to the presence of fine fibres. Since the fibre/matrix interface can act as a source of dislocations, the matrix can work-harden at a faster rate due to a decrease in the inter-fibre spacing. Thus the matrix strength at the composite fracture strain can be considerably greater than the strength of the same material without the presence of the reinforcing phase. Second, the fibre grown *in situ* by directional solidifcation are likely to contain surface defects which might lower the fracture stress of the fibres. Thus the rule of mixtures may either underestimate or overestimate the tensile strength of the composite. In the case of the Zn–Ge eutectic, the Ge fibres are very irregular and are not aligned in the growth direction. In spite of the misalignment and the lower volume fraction of the Ge fibres, the high tensile strength of the modified eutectic tends to indicate that the fibres are more perfect in nature than the corresponding Si fibres, and that the matrix strength is higher than the assumed value of 69 N mm^{-2} or 10 000 psi due to increased work-hardening.

Metallographic examination of longitudinal sections through the fractured surface of unmodified Zn–Ge eutectics showed some broken fibre segments close to the fracture surface. However, the cracking of the Ge dendrites near the fracture surface was not as extensive as in Al–Si eutectic alloy (see Fig. 4 in [51]). The breaking of the dendrites in tensile testing confirmed that there is at least some transfer of load from the zinc matrix to the Ge phase. The fracture surface of the modified eutectic, examined by SEM, showed elongated dimples of the matrix which is a common feature of the fracture surface of the unidirectionally solidifed eutectic composites [15, 21, 22].

3.3.2. Compressive properties

The nature of the variation of the compressive properties of the Zn–Ge eutectic was similar to those of its tensile properties. Highest strengths were obtained only in the modified conditions. This is contrary to the observations made in the case of Al–Si alloys where maximum compressive strength was obtained only at the slowest growth rate.

It was observed that, in common with the Al–Si eutectics, Zn–Ge specimens grown at freezing rates greater than $16\,\mathrm{mm\,h^{-1}}$, became barrel-shaped during compression. However, by lubricating the specimen ends with 0.05mm thick Teflon sheet to reduce frictional stresses between the ends of the specimen and the compression plates the tendency towards barrelling was eliminated. There was also a decrease in the compressive properties (yield and ultimate) when the specimen ends were lubricated.

Table I shows that for any growth rate the compressive yield and ultimate strengths are higher than the respective tensile properties. A similar difference to that observed in this work has been reported for other eutectics [5, 6, 15]. This is usually attributed to the difference in the coefficient of thermal expansion of the two phases. The thermal expansion coefficients for Ge (α_f) and Zn (α_m) are 6.0×10^{-6} and 34×10^{-6} $^\circ\mathrm{C}^{-1}$ respectively [14, 18, 23]. Since $\alpha_m > \alpha_f$ the residual stresses developed on cooling from the eutectic temperature are tensile in the zinc matrix and compressive in the Ge matrix. Thus the matrix will yield at a lower stress level in tension than in compression.

Shear mode buckling has been found to be a common feature in compression for some directionally solidified eutectics [24–26], and it has been confirmed that buckling is a concommittant of deformation and not a growth defect. The overall fracture surface of the Zn–Ge eutectic directionally solidifed at $2.7\,\mathrm{mm\,h^{-1}}$ was inclined at 45° to the axis of compression (Fig. 12). This optical micrograph shows the extensive shear mode buckling of the Ge phase near the fracture surface and little elsewhere. Specimens from other growth conditions did not fracture and testing was discontinued after the U.C.S. However, in these compressed specimens extensive non-localized buckling and fragmentation took place.

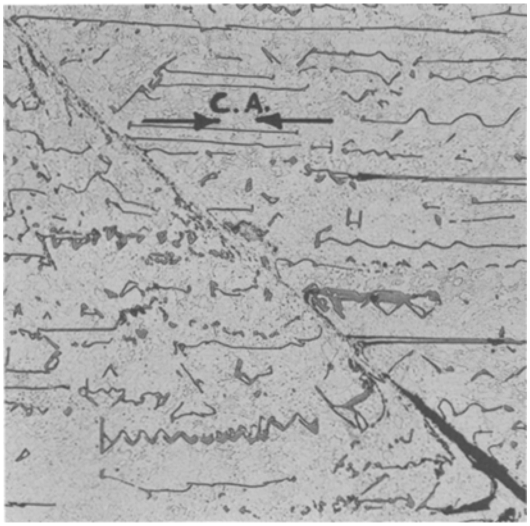

Figure 12 Optical micrograph of the compressive fracture surface of the Zn–Ge eutectic directionally solidified at $2.7\,\mathrm{mm\,h^{-1}}$ (× 100). (C.A. = compressive axis.)

Since the growth direction of the zinc at low growth rates is $\langle 0001 \rangle$, the shear fracture and low yield stress suggests that slip takes place relatively easily and on $\{11\bar{2}2\}$ throughout the entire cross-section of the specimen. In the case of Al–Si, no discernable texture was present in the aluminium phase and so the matrix was able to support shear strains more effectively. Thus the $\langle 100 \rangle$ silicon or germanium phase is only likely to provide marked compressional stiffness if the matrix can provide appropriate mechanical restraint on the plain containing the maximum resolved shear stress.

4. Conclusion

In common with the microstructure of the Al–Si eutectic, the morphology of Ge phase in the Zn–

Ge eutectic changes from a branched dendritic form at low growth rates to a modified fibrous form at extremely fast growth rates. Less than 0.05 wt% elemental sodium is able to change the coarse irregular flaky form of Ge to a modified fibrous form.

The effects of increasing growth rate on the room temperature tensile and compressive properties of the Zn–Ge eutectics are similar to those of the Al–Si eutectic. Although it contains only 7 vol% of the Ge phase highest strengths obtained in the modified condition are comparable to those of the Al–Si eutectic which contain 14.5 vol% of the Si phase. However, the prospect of producing eutectic alloys in this volume fraction group with the marked compressional stiffness of the Al–Si alloys, in which the silicon is present as ⟨100⟩ axial branched-dendrites, is unlikely unless the texture of its matrix phase if present at all, is such that appropriate lateral mechanical support is provided to the dendrites.

Acknowledgements

It is a pleasure to acknowledge the help and encouragement of Dr W. B. F. Mackay at Queen's University, Kingston, Canada. The work described here has been made possible via the financial support of the National Research Council of Canada.

References

1. M. N. CROKER, R. S. FIDLER and R. W. SMITH, *Proc. Roy. Soc.* **A335** (1973) 15.
2. M. N. CROKER, M. McPARLAN, D. BARAGAR and R. W. SMITH, *J. Crystal Growth* **29** (1975) 85.
3. M. N. CROKER, D. BARAGAR and R. W. SMITH, *ibid* **30** (1975) 198.
4. H. A. H. STEEN and A. HELLAWELL, *Acta. Met.* **20** (1972) 363.
5. M. SAHOO and R. W. SMITH, *Met. Sci.* **9** (1975) 217.
6. W. R. KRUMMHEUER and H. ALEXANDER, *J. Mater. Sci.* **9** (1974) 229.
7. M. G. DAY and A. HELLAWELL, *Proc. Roy. Soc.* **A305** (1968) 473.
8. A. HELLAWELL, *Prog. Mat. Sci.* **15** (1970) 1.
9. J. R. PATEL and B. H. ALEXANDER, *Acta Met.* **4** (1956) 385.
10. M. G. DAY and A. HELLAWELL, *J. Inst. Metals* **95** (1967) 337.
11. R. W. SMITH, "The Solidifcation of Metals",no. 110 (Iron and Steel Institute, 1968) p. 226.
12. W. J. McGREGOR TEGART, "Elements of Mechanical Metallurgy" (Macmillan, New York, 1966) p. 154.
13. N. R. RISEBROUGH, Ph.D. thesis, University of British Columbia, Canada (1964).
14. C. J. SMITHELS, "Metals Reference Book", 4th Edn. (Butterworth, London, 1967).
15. H. BIBRING, "Proceedings of the Conference on In-Situ Composites", Vol. II (National Academy of Science, 1972) p. 1.
16. M. M. FARAG and M. C. FLEMMING, *Met. Trans.* **6A** (1975) 1009.
17. W. KOSTER, *Z. Matallk* **39** (1948) 1.
18. M. E. FINE, *J. Appl. Phys.* **24** (1953) 338.
19. G. L. PEARSON, W. T. READ and W. L. FIELDMAN, *Acta Met.* **5** (1967) 181.
20. T. L. JOHNSON, R. J. STOKES and C. H. LI, *ibid* **6** (1958) 713.
21. M. J. SALKIND, F. D. LEMKEY and F. D. GEORGE, "Whisker Technology" edited by A. P. Levitt, (Interscience, New York, 1970) p. 343.
22. B. CANTOR, G. J. MAY and G. A. CHADWICK, *J. Mater. Sci.* **8** (1973) 830.
23. J. MEDERFF and I. CARDOFF, *Trans. Met. Soc. AIME* **230** (1964) 246.
24. B. J. SHAW, *Acta Met.* **15** (1967) 1169.
25. A. S. YUE, F. W. CROSSMAN, A. F. VIDOZ and M. I. JACOBSON, *Trans. Met. Soc. AIME* **242** (1968) 2441.
26. A. PATTANAIK and A. LAWLEY, *Met. Trans.* **2** (1971) 1529.

Received 31 July and accepted 2 December 1975.